The mechanism of magnetism in stacked nanographite: theoretical study

2001 J. Phys.: Condens. Matter 13 1295

(http://iopscience.iop.org/0953-8984/13/6/309)

INSTITUTE OF PHYSICS PUBLISHING JOURNAL OF PHYSICS: CONDENSED MATTER

J. Phys.: Condens. Matter **13** (2001) 1295–1302 www.iop.org/Journals/cm PII: S0953-8984(01)17851-3

The mechanism of magnetism in stacked nanographite: theoretical study

Kikuo Harigaya[1]

Physical Science Division, Electrotechnical Laboratory, Umezono 1-1-4, Tsukuba 305-8568, Japan[2],
National Institute of Materials and Chemical Research, Higashi 1-1, Tsukuba 305-8565, Japan
and
Kanazawa Institute of Technology, Ohgigaoka 7-1, Nonoichi 921-8501, Japan

E-mail: harigaya@etl.go.jp

Received 9 October 2000, in final form 15 December 2000

Abstract

Nanographite systems, where graphene sheets of dimensions of the order of nanometres are stacked, show novel magnetic properties, such as spin-glass-like behaviours and change of electron spin-resonance linewidths in the course of gas adsorptions. We investigate stacking effects in zigzag nanographite sheets theoretically, by using a tight-binding model with Hubbard-like on-site interactions. We find a remarkable difference in magnetic properties between the simple A–A-type and A–B-type stackings. For the simple stacking, there are no magnetic solutions. For the A–B stacking, we find antiferromagnetic solutions for strong on-site repulsions. The local magnetic moments tend to exist at the edge sites in each layer due to the large amplitudes of the wavefunctions at these sites. Relations with experiments are discussed.

1. Introduction

Nanographite systems, where graphene sheets of size of the order of nanometres are stacked, show novel magnetic properties, such as spin-glass-like behaviours [1] and change of ESR linewidths in the course of gas adsorptions [2]. Recently, it has been found [3] that magnetic interaction increases with the decrease of the interlayer distance, while water molecules are attached physically. Here, the change of the interlayer interactions has been anticipated experimentally, but theoretical studies have not been reported yet.

In this paper, we consider the stacking effects in zigzag nanographite sheets theoretically [4–6], by using a tight-binding model with Hubbard-like on-site interactions U. In the papers [4–6], one-dimensional graphite ribbons were investigated. In this paper, we assume that each graphite sheet has a hexagonal shape with zigzag edges. Such a shape geometry has been used in

[1] URL: http://www.etl.go.jp/~harigaya/; address after January 2001: National Institute of Advanced Industrial Science and Technology (AIST), Tsukuba 305, Japan.
[2] Correspondence address.

0953-8984/01/061295+08$30.00

the semi-empirical study of fluorine-doped graphite nanoclusters [7], too. Two stacking types, namely the A–A and A–B types, shown in figure 1 are considered in the model. We assume small interlayer interactions t_1 where two carbon atoms are adjacent between neighbouring layers. The circles in figure 1(a) (i.e., nanographite **a**) and figure 1(c) (nanographite **c**) show the sites with the interaction t_1, and the interaction t_1 is considered at all of the sites in figure 1(b) (nanographite **b**). Such interactions preserve the beautiful bipartite property seen in the single hexagonal layer.

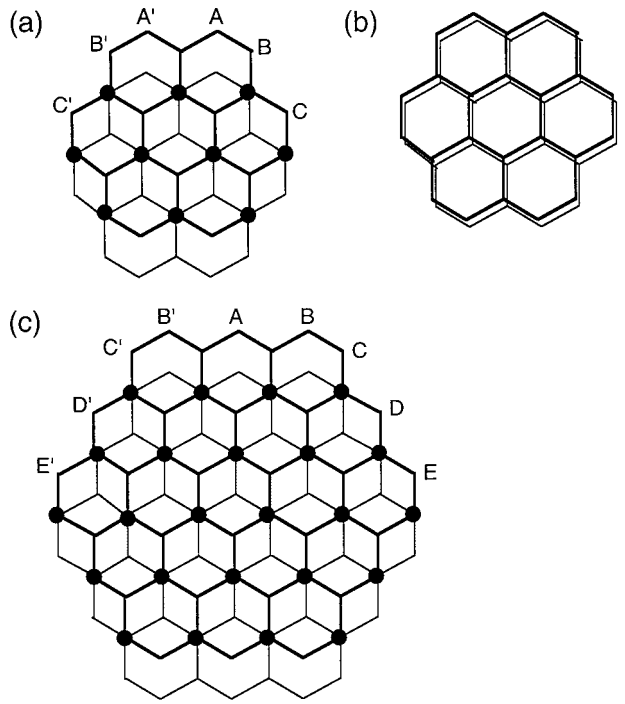

Figure 1. Stacked nanographite with zigzag edges. The bold and thin lines show the first and second layers, respectively. The stacking is of A–B type in (a) (nanographite **a**) and (c) (nanographite **c**), and it is of simple A–A type in (b) (nanographite **b**). There are 24 carbon atoms in one layer in (a) and (b), and there are 54 atoms in one layer in (c). The filled circles in (a) and (c) show lattice positions with small interlayer interactions t_1, and the bold symbols indicate some of the edge sites in the first layer. The sites, A (B, C, ...) and A′ (B′, C′, ...), are symmetrically equivalent, respectively.

The main finding of this paper is a remarkable difference in magnetic properties between the simple A–A and A–B stackings. For the simple stacking, we have not found magnetic solutions, because the presence of local magnetic moments is suppressed at the carbons. For the A–B stacking, we have found antiferromagnetic solutions for $U > 2t$, t being the hopping integral in a layer. The local magnetic moments tend to exist at the edge sites in each layer due to the large amplitudes of the wavefunctions at these sites. Relations with experiments are discussed extensively.

In section 2, we explain our model. Sections 3 and 4 are devoted to the total magnetic moment per layer, and the local magnetic polarization per site, respectively. In section 5, we discuss the local density of states at the edge carbon atoms. This paper is closed with a summary in section 6.

2. Model

We study the following model with integrals for hopping between orbitals of carbon atoms and on-site strong repulsions of the Hubbard type:

$$H = -t \sum_{\langle i,j\rangle:\,\text{intralayer}} \sum_{\sigma} (c^{\dagger}_{i,\sigma} c_{j,\sigma} + \text{h.c.}) - t_1 \sum_{\langle i,j\rangle:\,\text{interlayer}} \sum_{\sigma} (c^{\dagger}_{i,\sigma} c_{j,\sigma} + \text{h.c.}) + U \sum_{i} n_{i,\uparrow} n_{i,\downarrow} \tag{1}$$

where $n_i = c^{\dagger}_{i,\sigma} c_{i,\sigma}$ for $\sigma = \uparrow$ and $\downarrow$; $c_{i,\sigma}$ is an annihilation operator of an electron at the ith site with spin σ; the first sum is taken over the nearest-neighbour pairs $\langle i, j\rangle$ in a single layer of the nanographite; the third sum is taken over sites where the distance between the two positions of the neighbouring layers is shortest; t_1 is the strength of the weak hopping interaction between neighbouring layers; the positions of t_1 are shown by the filled circles in figure 1(a) (nanographite **a**) and figure 1(c) (nanographite **c**); the interaction t_1 is considered at all of the sites in figure 1(b) (nanographite **b**); and the last term of the Hamiltonian is the strong on-site repulsion with the strength U.

The finite-size system, whose spatial dimension and number of stacked layers are relevant to the structural unit of the activated carbon fibre (even the present size $\sim$10 Å is a little smaller than the experimental size $\sim$40 Å), is diagonalized numerically using the periodic boundary condition for the stacking direction, and we obtain two kinds of solution. One of them is a non-magnetic solution where up- and down-spin electrons are not polarized in each layer. This kind of solution can be found in weak-U cases. The other kind of solution is an antiferromagnetic solution, where the number of up-spin electrons is larger than that of down-spin electrons in the first layer, the number of down-spin electrons is larger than that of up-spin electrons in the second layer, and so on. This kind of solution is realized in strong-U regions. There will be cases of incommensurate spin-density waves, but we have not obtained such solutions, because we chose initial magnetic ordered states which are commensurate with the one-dimensional lattice in the stacking direction at the first stage of the numerical iteration process. We have discussed the antiferromagnetism in C_{60} polymers previously [8]. The same technique (unrestricted Hartree–Fock approximation) as was used in reference [8] is found to be effective in this paper, too.

The parameters are changed within the ranges $0 \leqslant t_1 \leqslant 0.5t$ and $0 \leqslant U \leqslant 10t$. The real value of t_1 is estimated to be about $0.1t$ at most, but we change this parameter for more extended regions in order to look at the behaviours of solutions in detail. The number of electrons is the same as the number of sites, assuming half-filling of electronic states. All of the quantities with the dimension of energy are reported in units of t ($\sim$2.0–3.0 eV).

3. Magnetic moment per layer

First, we consider the total magnetic moment per layer for the nanographites **a** and **b**. Figure 2 shows the absolute value of the total magnetic moment per layer as functions of t_1 and U. Figures 2(a) and 2(b) are for nanographite **a**, and figure 2(c) is for nanographite **b**. (See the figure caption for the value of U for each plot.) Figure 2(a) shows the overall variations of the magnetic moment. When U is small, there appears a finite magnetic moment for the values of t_1 larger than the threshold of the phase transition. At $U = 2.5t$, the magnetic moment changes as a parabolic function with respect to t_1. The magnetic moment decreases for larger U: $U = 3.0t$, $5.0t$, and $10.0t$. This is due to the strong singlet correlation at the bonds t_1 with respect to the change of the Heisenberg coupling between the neighbouring layers as t_1^2/U. Figure 2(b) shows the details around the phase transition for $1.8t \leqslant U \leqslant 2.3t$. With

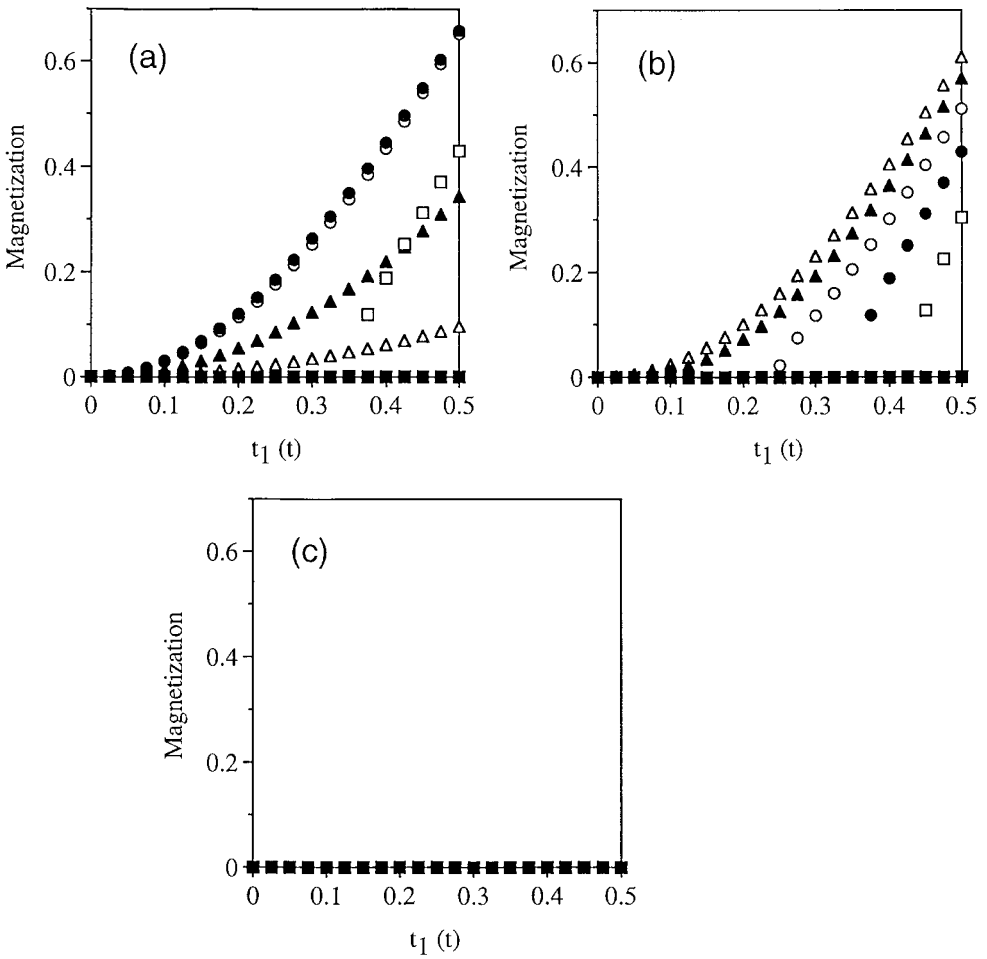

Figure 2. The magnitude of the total magnetic moment per layer as functions of t_1 and U. Parts (a) and (b) are for nanographite **a**, and part (c) is for nanographite **b**. In (a), the values of U are $U = 1.5t$ (filled squares), $2.0t$ (open squares), $2.5t$ (filled circles), $3.0t$ (open circles), $5.0t$ (filled triangles), and $10.0t$ (open triangles). Part (b) shows the details around the phase transition: the values of U are $U = 1.8t$ (filled squares), $1.9t$ (open squares), $2.0t$ (filled circles), $2.1t$ (open circles), $2.2t$ (filled triangles), and $2.3t$ (open triangles). In (c), the magnetic moment is zero for $0 \leqslant U \leqslant 10t$.

increasing U, the magnitude of the magnetization increases. The magnetic moment is zero in the smaller-t_1 region for $U = 1.8t$, $1.9t$, $2.0t$, and $2.1t$. The magnetic moment is zero only at $t_1 = 0$ for $U = 2.2t$ and $2.3t$. We can understand the parabolic curves as indicating a change due to the Heisenberg coupling proportional to t_1^2/U. The antiferromagnetic solutions actually exist for larger-U regions in the A–B stacking case. On the other hand, figure 2(c) shows the magnetic moment for the simple stacking. There is no magnetization for $0 \leqslant t_1 \leqslant 0.5t$ and $0 \leqslant U \leqslant 10t$. This absence of magnetization is related to the non-magnetic solution for the single nanographite sheet. The magnetic solution for the single sheet is not favoured in the A–A stacking case. This shows a remarkable difference between the simple A–A and A–B stackings, and is a new finding of this paper. There is no clear evidence as regards which stacking is realized experimentally [3]. However, we believe that the A–B stacking should exist

in nanographite systems because exotic magnetisms have been observed in recent experiments [1–3]. The increase of the magnetic interaction during attachment of water molecules [3] is induced by the decrease of the interlayer distance, which enhances the interaction strength t_1.

Next, figure 3 shows the absolute value of the magnetic moment per layer for nanographite **c** with A–B stackings. The number of carbons in a layer is 54, and this is more than twice as large as that for nanographite **a**. Figure 3(a) shows the change of the magnetic moment for wide parameter regions, and figure 3(b) displays the numerical data around the phase transition. The overall behaviours for smaller and larger U seem similar to those of figure 2. The characteristic value of U decreases from that of figure 2. For example, the curve becomes parabolic for $U \geqslant 2.2t$ in figure 2(b), and it becomes parabolic for $U \geqslant 2.0t$ in figure 3(b). Such quantitative difference is due to the effects of the larger system size.

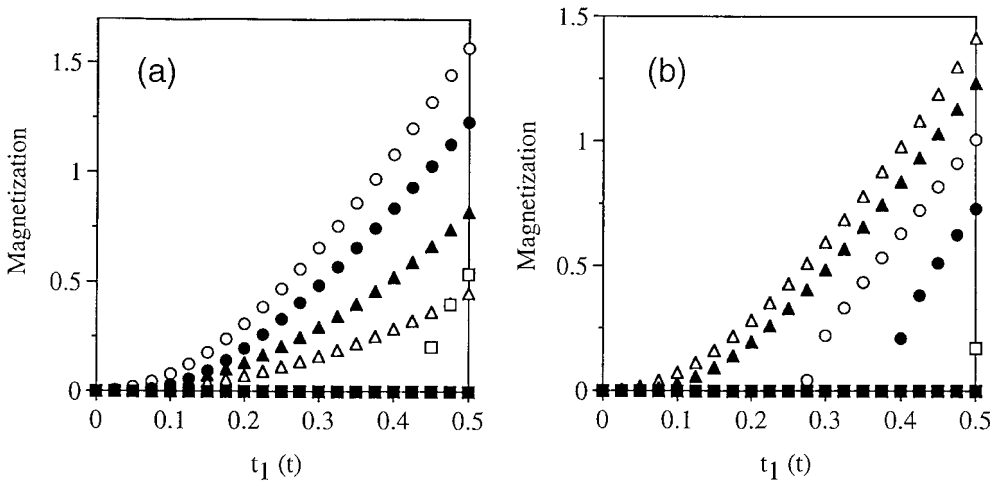

Figure 3. The magnitude of the total magnetic moment per layer as functions of t_1 and U for nanographite **c**. In (a), the values of U are $U = 1.0t$ (filled squares), $1.5t$ (open squares), $2.0t$ (filled circles), $2.5t$ (open circles), $5.0t$ (filled triangles), and $7.0t$ (open triangles). Part (b) shows the details around the phase transition: the values of U are $U = 1.2t$ (filled squares), $1.4t$ (open squares), $1.6t$ (filled circles), $1.8t$ (open circles), $2.0t$ (filled triangles), and $2.2t$ (open triangles).

4. Local magnetic polarization in a layer

In order to give further insight into the mechanism of the magnetism, we will look at the local magnetic moments which depend on the carbon sites in each layer. We particularly pay attention to the local magnetism near the edge sites of the nanographite [4–6].

Figure 4 shows the local magnetic moment at the edge sites of nanographite **a**. The values of U are $U = 2.1t$ and $2.5t$ in figures 4(a) and 4(b), respectively. In the former case, there is a point of phase transition near $t_1 = 0.25t$, and a finite magnetization appears for non-zero t_1 in the latter case. The filled squares, open squares, and filled circles show the results at sites A, B, and C, respectively. Due to the symmetry, the magnetic moments at the sites A′, B′, and C′ of figure 1(a) are equal to those of the sites A, B, and C. Figure 5 displays similar plots for nanographite **c**. The parameters are $U = 1.8t$ and $2.5t$ in figures 5(a) and 5(b), respectively. We see that the local magnetic moment is negative along the edge A–A′ in figure 1(a), and also along the edge A–B–A′ in figure 1(c). The local magnetic moment is positive along the neighbouring edges: namely, the edges B–C and B′–C′ in figure 1(a), and the edges C–D–E

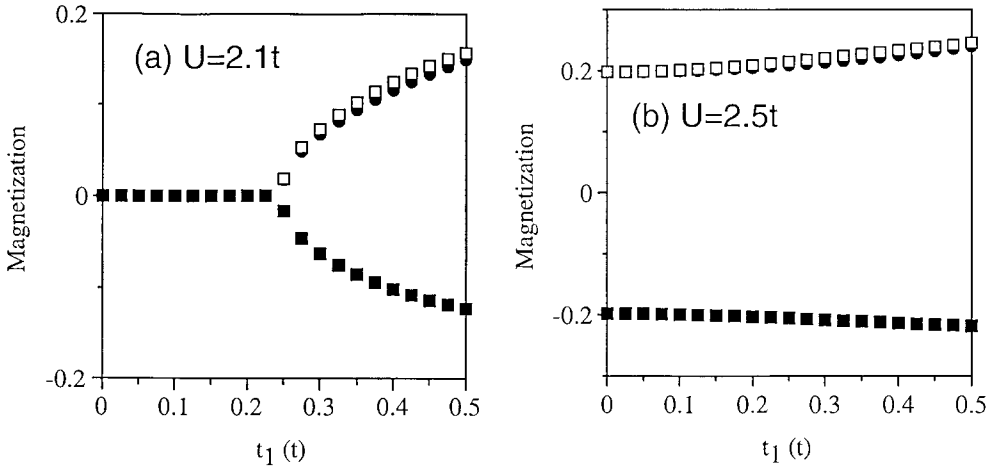

Figure 4. The local magnetic moment at the edge sites of nanographite **a**. The values of U are $U = 2.1t$ in (a), and $2.5t$ in (b). The filled squares, open squares, and filled circles show the results for sites A, B, and C, respectively.

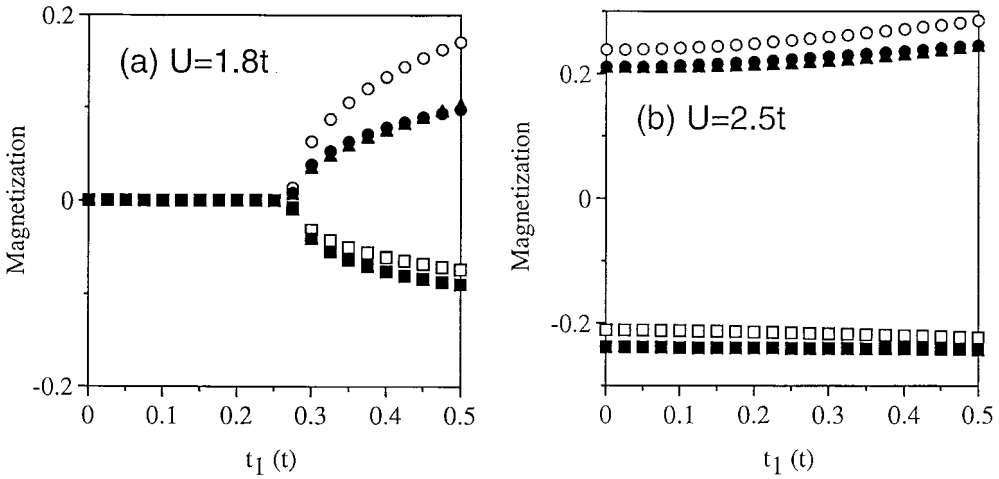

Figure 5. The local magnetic moment at the edge sites of nanographite **c**. The values of U are $U = 1.8t$ in (a), and $2.5t$ in (b). The filled squares, open squares, filled circles, open circles, and filled triangles show the results for sites A, B, C, D, and E, respectively.

and C′–D′–E′ in figure 1(c). Such positive/negative alternations of magnetic moments are seen in the calculations for both nanographites **a** and **c**. Because there are strong amplitudes of the wavefunctions at the zigzag edge sites [4–6], the local moments near these edge carbon atoms tend to become larger. In the A–B stackings, there is no interlayer interaction t_1 at the edge sites, and this gives rise to the finite magnetic moment per layer which was discussed in the previous section. On the other hand, the local magnetic moment and also the magnetic moment per layer do not appear in the simple A–A stacking case, namely that of nanographite **b** of figure 1(b), owing to the interlayer interactions t_1 which are present between all the nearest carbon atoms of neighbouring layers. This difference is the origin of the lack of magnetization in the simple stacking case reported in figure 2(c).

In the band calculations for the stacked nanographite ribbons [9], the strong hybridization between edge states occurs in the A–A stacking case. Such hybridization is weak in the A–B stacking case. The strong localization of wavefunctions at the edge carbon sites persists in the band calculations for systems with the A–B stacking [9], and this property agrees with the present result.

5. Density of states

In this section, we discuss the local density of states at the edge sites. The wavefunctions of electrons with up and down spins are projected on the edge sites of nanographite **a** and **c**. The local density of states is reported together with the total density of states.

Figure 6 shows the density of states of nanographite **a**, and figure 7 displays the result for nanographite **c**. The total density of states per layer and per spin is shown by the bold line. The local density of states at the edge sites is shown by the thin and dashed lines for the up and down spins, respectively. The up and down splitting typical for antiferromagnetism is seen in both figures. Because the number of edge sites is one third of the total number of carbon atoms in nanographite **a**, the areas between the lines and the horizontal axis also have this relative ratio. In nanographite **c**, the proportion of number of edge sites with respect to total number of carbon atoms becomes smaller. Therefore, the relative area below the thin and dashed lines becomes smaller in figure 7. In one-dimensional graphite ribbons [4–6], there appears a strong peak due to the localized edge states at the Fermi energy. This is seen in the non-interacting case. With interactions taken into account, such edge states split into bonding (occupied) and antibonding (unoccupied) states. This will be one of the reasons that such a strong peak is not observed in figures 6 and 7. Also, in the present case, the edge sites do not make a one-dimensional lattice and each layer has a finite spatial dimension. This difference is another reason for the absence of a strong peak.

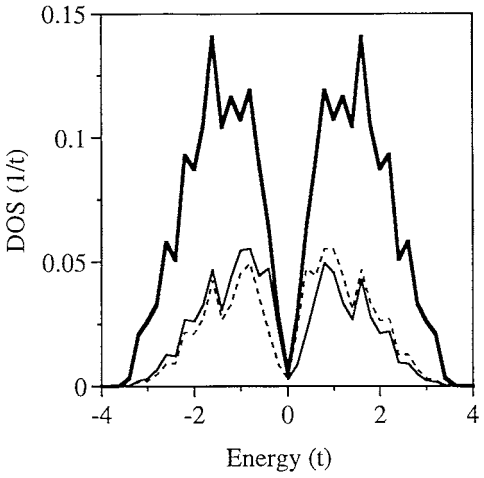

Figure 6. The density of states per layer for nanographite **a**. The parameters are $t_1 = 0.4t$ and $U = 2.1t$. The bold line shows the density of states over 24 carbon atoms per layer and per spin. The thin and dashed lines indicate the densities of states over the eight edge sites in a layer for the up and down spins, respectively.

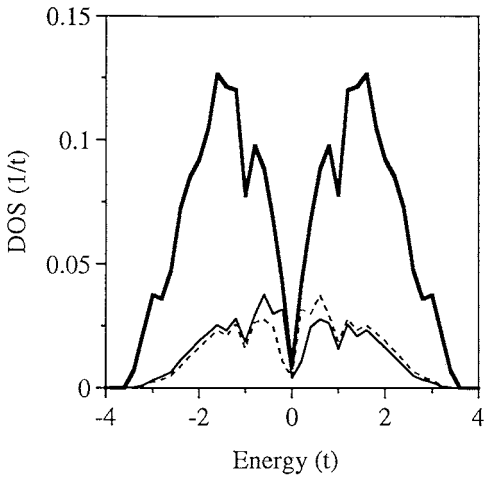

Figure 7. The density of states per layer for nanographite **c**. The parameters are $t_1 = 0.4t$ and $U = 1.8t$. The bold line shows the density of states over 54 carbon atoms per layer and per spin. The thin and dashed lines indicate the densities of states over the twelve edge sites in a layer for the up and down spins, respectively.

6. Summary

In summary, we have investigated the stacking effects in zigzag nanographite sheets theoretically. We have found a remarkable difference in magnetic properties between the simple A–A-type and A–B-type stackings. For the simple stacking, there are no magnetic solutions. For the A–B stacking, we find antiferromagnetic solutions for strong on-site repulsions. The local magnetic moments exist at the edge sites due to the large amplitudes of the wavefunctions at the zigzag edge sites. The A–B-type stacking is favourable to the observation of exotic magnetism in nanographite systems.

Acknowledgments

The author is grateful for interesting discussions with T Enoki, T Kawatsu, H Sato, T Ohshima, Y Miyamoto, K Kusakabe, K Nakada, K Wakabayashi, and M Igami. Useful discussions with the members of the Condensed Matter Theory Group (http://www.etl.go.jp/˜theory/), Electrotechnical Laboratory, is acknowledged, too.

References

[1] Shibayama Y, Sato H, Enoki T and Endo M 2000 *Phys. Rev. Lett.* **84** 1744
[2] Kobayashi N, Enoki T, Ishii C, Kaneko K and Endo M 1998 *J. Chem. Phys.* **109** 1983
[3] Kawatsu N, Sato H, Enoki T, Endo M, Kobori R, Maruyama S and Kaneko K 2000 *Meeting Abstracts of the Physical Society of Japan* vol 55, issue 1 (Tokyo: The Physical Society of Japan) p 717
[4] Fujita M, Wakabayashi K, Nakada K and Kusakabe K 1996 *J. Phys. Soc. Japan* **65** 1920
[5] Fujita M, Igami M and Nakada K 1997 *J. Phys. Soc. Japan* **66** 1864
[6] Nakada K, Fujita M, Dresselhaus G and Dresselhaus M S 1996 *Phys. Rev.* B **54** 17954
[7] Saito R, Yagi M, Kimura T, Dresselhaus G and Dresselhaus M S 1999 *J. Phys. Chem. Solids* **60** 715
[8] Harigaya K 1996 *Phys. Rev.* B **53** R4197
[9] Miyamoto Y, Nakada K and Fujita M 1999 *Phys. Rev.* B **59** 9858